Continental J. Applied Sciences
Omoniyi et al. (2026) 21 (3): 22 – 48 Doi: 10.5281/zenodo.19454197

Review Article

Autonomous Multi-Sensor Air Quality Monitoring System for Abattoirs and Waste Environments: Development and Performance Evaluation

Olatunji Omoniyi[1,2], Christopher O. Akinbile[1] Jide J. Popoola[3] Victoria O.E. Akpambang[4]
[1]Department of Agricultural and Environmental Engineering, Federal University of Technology, Akure, Nigeria.
[2]Department of Agricultural and Bio-Environmental Engineering, Federal College of Agriculture, Akure, Nigeria
[3]Department of Electrical and Electronics Engineering, Federal University of Technology, Akure, Nigeria.
[4]Department of Chemistry, Federal University of Technology, Akure, Nigeria.
Corresponding email: omoniyiolatunji007@gmail.com

Abstract

This study reports the development and validation of a low-cost, autonomous multi-sensor device for monitoring gaseous and particulate emissions in waste management and livestock processing environments. The platform integrates electrochemical, metal-oxide semiconductor (MOS), and optical sensors to measure CO, CO_2, CH_4, NH_3, H_2S, NO_2, SO_2, H_2, acetone, TVOCs, and particulate matter (PM_1, $PM_{2.5}$, PM_{10}), together with temperature, relative humidity, and wind speed. To support reliable long-term outdoor deployment, the system was built with dual IP65-rated enclosures, SD card data logging, GSM-based data transmission, and watchdog-protected firmware. Calibration using certified gases, aerosol chambers, and reference instruments produced strong sensor responses, with coefficients of determination (R^2) ranging from 0.92 to 0.99 across the monitored parameters. The power subsystem, comprising an 18 Ah, 12 V sealed lead-acid battery and a 30 W photovoltaic panel, sustained off-grid operation for more than 51 hours, while sensitivity analysis indicated that optimized duty-cycling of high-consumption components could extend autonomy to about 72 hours. Field deployments further demonstrated stable operation across wet and dry seasons, minimal zero-drift, and a positive daily energy balance under an average device load of about 4.2 W. These results confirm the system's suitability for continuous, real-time emission profiling and microclimate monitoring in abattoirs, landfills, and other emission-prone environments. The developed platform, therefore, provides a scalable and cost-effective tool for exposure assessment, environmental risk management, regulatory surveillance,

ISSN: 3043-6087. Science and Education Development Inst., Nigeria

and compliance monitoring in relation to WHO air quality guidelines and national environmental standards. Broader adoption will benefit from routine calibration, adaptive power optimization, and dashboard-based visualization to strengthen evidence-based environmental policy and occupational health interventions.

Keywords: Autonomous multi-sensor device; air quality monitoring; gaseous and particulate emissions; low-cost sensors; abattoirs and waste management; real-time environmental monitoring.

Received: 14 January 2026 **Accepted: 05 April 2026**

Citation: Omoniyi, O., Akinbile, C.O., Popoola, J.J., Akpambang, V.O.E. (2026). Autonomous Multi-Sensor Air Quality Monitoring System for Abattoirs and Waste Environments: Development and Performance Evaluation. Continental J. Applied Sciences, 21(3), 22-48. Doi: 10.5281/zenodo.19454197

Introduction

Air pollution from semi-mechanized abattoirs represents an emerging environmental and public health challenge in rapidly urbanizing regions of Nigeria. These facilities are integral to the meat supply chain but generate significant gaseous and particulate emissions due to animal slaughter, by-product decomposition, and inadequate waste management practices (Ogunjuyigbe et al., 2020; Akinmolayan et al., 2021). Common pollutants include carbon monoxide (CO), carbon dioxide (CO_2), methane (CH_4), ammonia (NH_3), hydrogen sulfide (H_2S), nitrogen dioxide (NO_2), sulfur dioxide (SO_2), volatile organic compounds (VOCs), and airborne particulate matter (PM_1, $PM_{2.5}$, PM_{10}). Exposure to these emissions has been linked to occupational health risks for abattoir workers, nuisance odours in nearby communities, and greenhouse gas emissions that exacerbate climate change (Ni et al., 2017; Hristov et al., 2018; WHO, 2022).

While several studies have characterized environmental contamination associated with waste and industrial activities in Nigeria, including impacts on soil and groundwater quality and pollutant accumulation in surrounding media (Akinbile, 2012; Akpambang et al., 2022), there remains a gap in the quantitative assessment of gaseous emissions and airborne particulates from such facilities. Air quality monitoring in Low- and Middle-Income Countries (LMICs) is limited by the high cost of reference-grade instruments, sparse regulatory infrastructure, and the need for continuous monitoring in diverse microenvironments (Castell et al., 2017; Ajayi and Tukur, 2022). Traditional monitoring stations are ill-suited to abattoir environments because they are expensive, require controlled conditions, and cannot be easily deployed near emission sources. Recent advances in low-cost sensing technology, such as electrochemical and metal-oxide semiconductor (MOS) sensors, have created opportunities for distributed, real-time monitoring of multiple pollutants at relatively low power consumption (Spinelle et al., 2015; Nadimi and Blanes-Vidal, 2019). Integrating these sensors into compact, robust devices offers a path toward capturing high-resolution temporal and spatial data necessary for exposure assessment, risk characterization, and policy development (Lewis et al., 2016; Burt, 2022).

This study reports the development and validation of a multi-sensor air-monitoring device tailored for deployment in semi-mechanised abattoirs in Akure, Nigeria. The device integrates electrochemical, MOS, and optical sensors to simultaneously measure CO, CO_2, CH_4, NH_3, H_2S, NO_2, SO_2, H_2, acetone, TVOCs, and particulate matter, alongside meteorological parameters such as temperature, relative humidity, and wind speed. The system emphasizes accuracy, durability, low power consumption, and autonomous operation under challenging field conditions. By providing synchronized, high-resolution emission data, the device supports evidence-based interventions, regulatory compliance with NESREA standards, and alignment with global frameworks such as the WHO Air Quality Guidelines and Sustainable Development Goals (SDGs 3 and 13) (Odhiambo et al., 2021; Morin et al., 2022).

Materials and Methods

Device Design and Development with enclosure

A multi-sensor monitoring device was designed and constructed to quantify emissions from semi-mechanized abattoirs and other waste sites in Akure, Nigeria. The device integrates electrochemical, metal-oxide semiconductor (MOS), and optical sensors to measure gaseous pollutants carbon monoxide (CO), carbon dioxide (CO_2), methane (CH_4), ammonia (NH_3), hydrogen sulfide (H_2S), nitrogen dioxide (NO_2), sulfur dioxide (SO_2), hydrogen (H_2), acetone (C_3H_6O), and total volatile organic compounds (TVOCs) alongside particulate matter (PM_1, $PM_{2.5}$, PM_{10}), temperature, relative humidity (RH), and wind speed. These parameters were selected to capture the emissions and microclimatic conditions characteristic of abattoir operations, which influence pollutant generation and dispersion (Piedrahita et al., 2014; Castell et al., 2017).

The device was designed for accuracy, durability, low power consumption, and field portability. It features GPS-enabled geo-tagging and cloud-based data transmission for real-time analysis and hotspot mapping. The developed device is being enclosed inside two carefully selected plastic enclosures to prevent moisture and dust ingress

Sensor Selection and Specifications

Each sensor was chosen based on sensitivity, detection range, selectivity, environmental robustness, power efficiency, and long-term stability (Nadimi and Blanes-Vidal, 2019; Kaur and Singh, 2021). Key components include: The device integrates multiple sensing modules selected for their precision and robustness in abattoir environments. Carbon monoxide was measured using the SPEC 110-102 electrochemical sensor with a detection

ISSN: 3043-6087. Science and Education Development Inst., Nigeria

range of 1–1000 ppm, offering fast response, low cross-sensitivity, and suitability for

combustion by-products (Chen et al., 2021; Adegbite et al., 2022). Carbon dioxide concentrations were monitored using the Senseair S8, a non-dispersive infrared (NDIR) sensor operating between 400–2000 ppm with ±(30 ppm) accuracy, widely validated for livestock and waste decomposition studies (Zhang et al., 2020; Akinmolayan et al., 2021). Methane detection employed the Figaro TGS2611, which uses catalytic bead or NDIR-based technology and is commonly used in landfill and livestock emission studies (Sun et al., 2019; Okeke et al., 2022). Particulate matter (PM_1, $PM_{2.5}$, PM_{10}) was measured by the Plantower PMS5003 laser-scattering sensor, known for its sensitivity to fine particles and use in health-relevant air quality monitoring (Li et al., 2021; WHO, 2022; Suriano and Prato, 2023). Ammonia and hydrogen sulfide were measured using MQ-137 and MQ-136 electrochemical/MOS sensors, which are reliable for odorous and hazardous gas detection in waste management facilities (Hristov et al., 2018; Ogunbode *et al*., 2021; Oyeleke et al., 2020). Nitrogen dioxide and sulfur dioxide were detected using the Alphasense NO_2-B43F and SO_2-B4 electrochemical sensors, offering ppb-level detection and high stability under outdoor conditions (Martinez et al., 2019; Spinelle et al., 2015). Acetone and total volatile organic compounds were monitored using the Winsen ZE25-VOC and Sensirion SGP30 digital MOS sensors, which are effective for odor profiling and occupational exposure assessments (Lee et al., 2020; Park et al., 2021), hydrogen emissions from anaerobic zones were monitored using the Figaro TGS821 MOS sensor, which provides rapid response and safety-critical leak detection (Sun et al., 2019). Environmental sensors such as Temperature (Pt100 RTD), RH (HYGROMER HT-1), and wind speed (RK100-02) were included to provide meteorological context for emission dispersion and transformation (Davis et al., 2019; Grayson and Connelly, 2021; Flemming, 2022). These measurements are essential for spatio-temporal modeling and compliance evaluation.

Microcontroller Architecture
The device employs an **Arduino Uno (ATmega328P)** for sensor integration, real-time acquisition, and communication. It's 32 KB flash memory stores firmware, SRAM buffers real-time data, and EEPROM retains calibration constants. Analog (A0–A5) and digital I/O pins interface with sensors; SPI supports SD card logging, I^2C connects multi-sensor modules, and UART communicates with GPS/GSM modules. Watchdog timers ensure reliability during long-term deployment (Flemming, 2022).

Data Flow and System Architecture
Signals from analog and digital sensors are processed by the ATmega328P ADC and firmware, averaged, converted using stored calibration coefficients, and logged to SD. Data packets are timestamped and optionally transmitted via GSM/Wi-Fi to a cloud server for remote analysis and visualization (Park et al., 2021).

Table 1: Design Considerations for Selected Sensors

Sensor	Key Considerations
CO (SPEC 110-102)	High sensitivity (ppm), stable calibration, low power
CO_2 (Senseair S8)	Accurate at low levels, power-efficient, long-term stability
CH_4 (TGS2611)	Sensitive at ppm, robust, low cross-sensitivity
$PM_1/PM_{2.5}/PM_{10}$ (PMS5003)	High accuracy, low maintenance
NH_3 (MQ-137)	Robust under humidity fluctuations, low energy requirement
H_2S (MQ-136)	Accurate at low ppm, corrosion-resistant
NO_2 (Alphasense B43F)	Detects ppb levels, minimal interference
SO_2 (Alphasense SO_2-B4)	High sensitivity, reliable under combustion conditions
Acetone (ZE25-VOC)	Digital output, low cross-sensitivity
TVOCs (SGP30)	Multi-VOC sensitivity, compensated for temp/RH
H_2 (TGS821)	Fast response, robust in anaerobic environments
Pt100 (Temperature)	±0.05 °C precision, outdoor durability
RH (HYGROMER HT-1)	±1% RH accuracy, long-term stability
Wind (RK100-02)	Accurate low-wind detection, rapid response

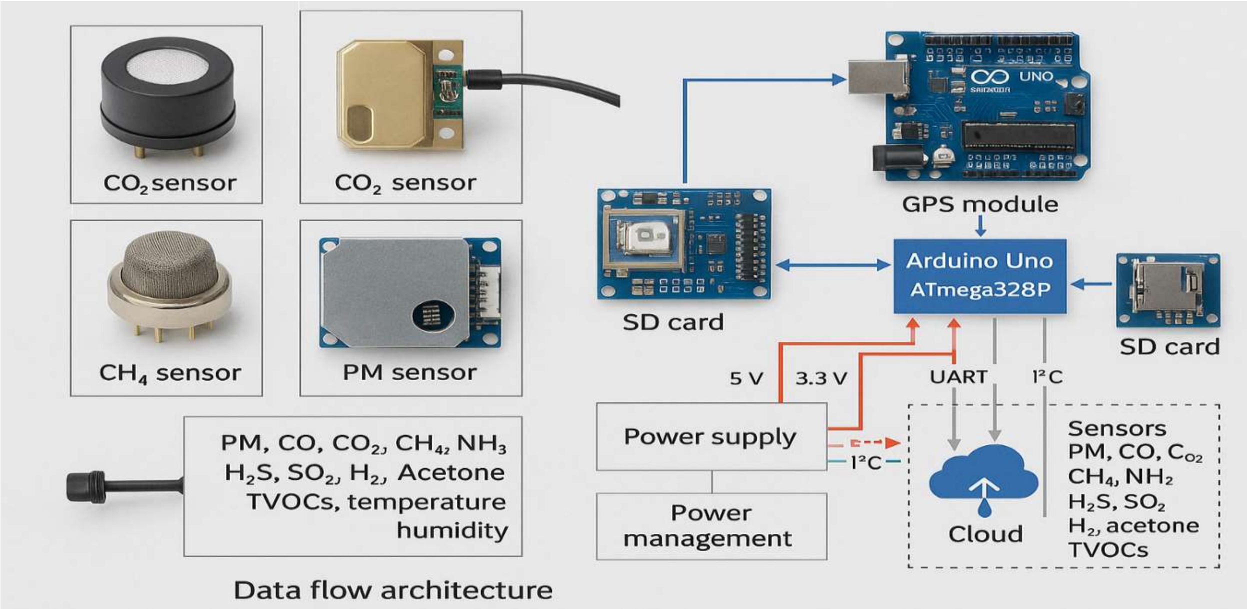

Figure 1: *Composite schematic and component collage of the multi-sensor monitoring device.*

ISSN: 3043-6087. Science and Education Development Inst., Nigeria

Figure 1 illustrates the physical hardware and system architecture. The left panel shows representative sensor modules, including CO_2 (NDIR), CH_4 (MOS), and particulate matter (PM_1/$PM_{2.5}$/PM_{10}) sensors, which collectively detect emissions from semi-mechanized abattoir operations. The integrated sensor suite monitors PM, CO, CO_2, CH_4, NH_3, H_2S, SO_2, H_2, acetone, TVOCs, temperature, and relative humidity. The right panel presents the data flow architecture: sensor signals are transmitted to an Arduino Uno (ATmega328P), which processes and calibrates data in real time, logs them to an SD card, and synchronizes geo-coordinates via a GPS module. Data are subsequently transmitted to the cloud via UART/I^2C communication for remote access, visualization, and hotspot mapping. Power management ensures stable 5 V and 3.3 V supplies for mixed-voltage sensor operation, enabling reliable, autonomous 24-hour deployment in field conditions.

Design Calculations

Design calculations were performed to verify the suitability of the developed monitoring platform for continuous field deployment, with emphasis on power demand, battery sizing, signal conditioning, data throughput, and thermal stability. The total current requirement of the integrated sensing and control system was estimated by summing the current draws of all sensors and the Arduino Uno, giving a total current of 0.435 A at 5 V. The corresponding system power demand was calculated as:

$$P_{total} = V\, I_{total} \quad (1)$$

$$P_{total} = 5 \times 0.435 = 2.18 \text{ W} \quad (2)$$

The minimum daily energy requirement for 24 h of uninterrupted operation was estimated from the computed system power as:

$$E_{24} = P_{total} \times t \quad (3)$$

$$E_{24} = 2.18 \times 24 = 52.32 \text{ Wh} \quad (4)$$

$$E_{battery} = V_{battery} \times C_{battery} \quad (5)$$

$$E_{battery} = 12 \times 18 = 216 \text{ Wh} \quad (6)$$

Although this value represents the theoretical minimum daily energy demand, battery selection was based on the need to accommodate regulator losses, depth-of-discharge limitations, short-term load fluctuations, battery ageing, and reduced solar input during unfavourable weather conditions. On this basis, an 18 Ah, 12 V sealed lead-acid (SLA) battery was selected. This energy reserve provides substantial operational margin above the minimum requirement and is consistent with recommended design practice for autonomous IoT-based environmental monitoring systems operating under variable outdoor conditions (Li et al., 2021; Nadimi and Blanes-Vidal, 2019).

Signal conditioning requirements were also incorporated into the design analysis. Raw sensor outputs were converted to engineering units using linear or polynomial calibration relationships, depending on the response characteristics of each sensing element (Sedra and Smith, 2020). For example, the carbon monoxide sensor response was represented as:

$$V_{out} = S[CO] \quad (7)$$

$$V_{out} = 30 \times 200 = 6000 \text{ mV} = 6 \text{ V} \quad (8)$$

Since this exceeds the 0–5 V analog-to-digital conversion range of the Arduino Uno, signal conditioning through voltage division and operational amplifier scaling was required to preserve measurement resolution and minimize conversion error (Sedra and Smith, 2020).

The expected data generation rate was estimated for 14 sensing channels, each producing 10 bytes per record at a sampling interval of 5 s, equivalent to 0.2 Hz. The data rate was therefore calculated as:

$$R_{data} = N \times B \times f \quad (9)$$

where N denotes the number of sensor channels, B the number of bytes recorded per channel per sample, and f the sampling frequency.

$$R_{data} = 14 \times 10 \times 0.2 = 28 \text{ bytes s}^{-1} \quad (10)$$

$$D_{day} = R_{data} \times 86400 \quad (11)$$

$$D_{day} = 28 \times 86400 = 2{,}419{,}200 \text{ bytes day}^{-1} \approx 2.42 \text{ MB day}^{-1} \quad (12)$$

This data volume is well within the capacity of the SD card module and remains suitable for low-energy GSM-based transmission in remote monitoring applications (Stallings, 2015; Park et al., 2021). Thermal performance was assessed by estimating an internal heat load of 0.65 W, corresponding to a predicted enclosure temperature rise of less than 10 °C above ambient. To minimise thermally induced sensor drift and maintain measurement stability, passive ventilation openings were incorporated into the enclosure design (Kraus and Aziz, 2001). Collectively, these calculations established the engineering basis for battery selection, analog front-end design, storage planning, and enclosure configuration, thereby supporting reliable long-term emission monitoring under field conditions.

ISSN: 3043-6087. Science and Education Development Inst., Nigeria

Calibration and Validation

All sensors were calibrated prior to field deployment using certified gases, aerosol chambers, and standard reference instruments to establish relationships between raw sensor outputs and engineering units (Shah and Kumar, 2020; Li et al., 2021). Gas sensors were first zeroed under clean-air conditions and then exposed stepwise to known concentrations across their intended operating ranges. Particulate matter sensors were calibrated by side-by-side comparison with a reference aerosol monitor under controlled loading conditions. Temperature, relative humidity, and wind speed sensors were similarly checked against laboratory and field standards. Calibration equations were derived using linear or polynomial regression, depending on sensor response characteristics, and the resulting coefficients were embedded in the firmware and stored in EEPROM for real-time correction during field measurements.

Software and Data Handling

The device firmware was developed in C++ using the Arduino IDE to manage sensor initialization, data acquisition, signal conversion, storage, and transmission. During startup, the control routine initialized all sensing modules, communication interfaces, and storage protocols. Thereafter, the main program executed continuous sampling, applied calibration equations to raw sensor outputs, and formatted the processed data for local logging and remote transmission. Measurements were stored on an SD card with corresponding timestamps and sensor identifiers to ensure traceability, while GSM-based communication enabled periodic cloud upload for external access and analysis. Watchdog timer routines were incorporated to reset the system automatically in the event of communication or processing faults, thereby supporting reliable long-term autonomous deployment (Stallings, 2015).

Results and Discussion

Device Architecture and System Integration

Field deployment confirmed the successful integration of the electrochemical, MOS, and optical sensing modules with the Arduino Uno (ATmega328P)-based control architecture. The assembled platform achieved synchronized acquisition of gaseous, particulate, and microclimatic data, while simultaneously supporting onboard SD-card logging, GPS-linked record generation, and GSM-enabled data transmission (Figure 2). Throughout wet- and dry-season operation, the system maintained uninterrupted measurement and data-handling functionality, indicating effective coordination among the sensing, processing, storage, and telemetry subsystems. These observations demonstrate that the developed architecture was sufficiently robust for autonomous, real-time monitoring under outdoor abattoir conditions, consistent with the growing applicability of compact low-cost sensing platforms in resource-constrained monitoring

ISSN: 3043-6087. Science and Education Development Inst., Nigeria

environments (Burt, 2022; Odhiambo et al., 2021).

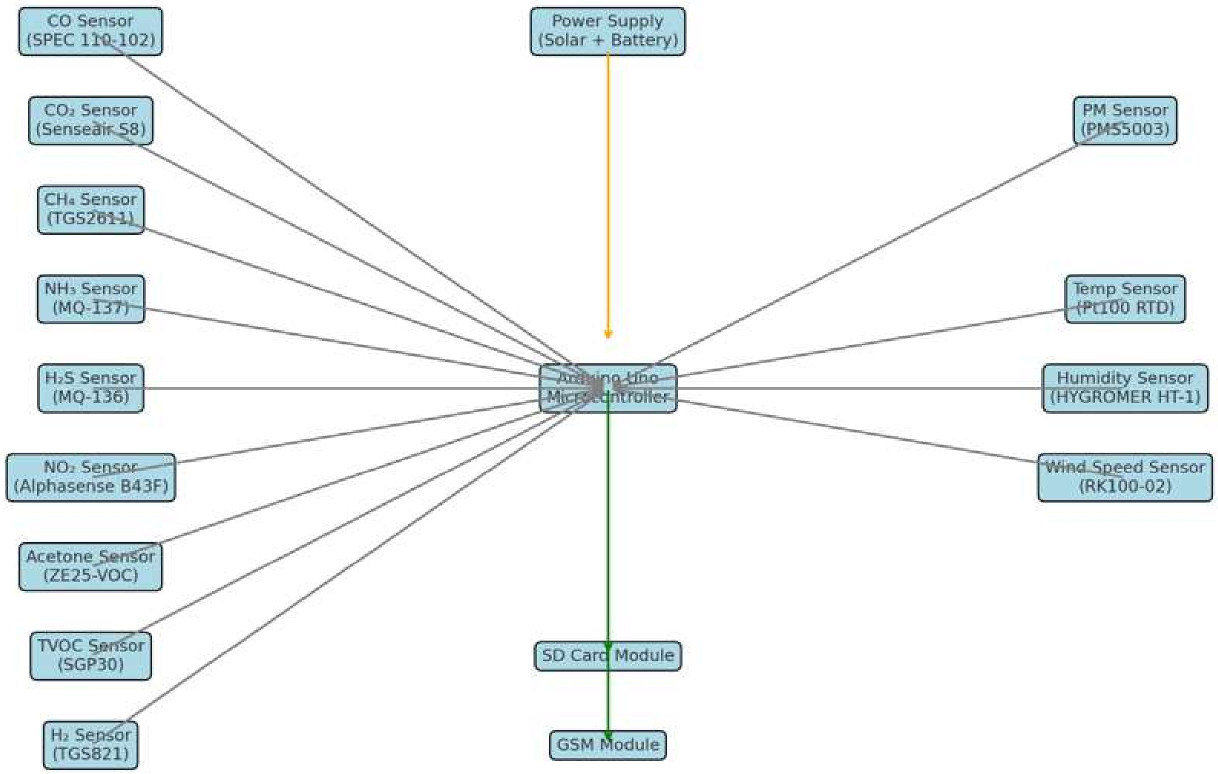

Figure 2: System Architecture of the Multi-sensor Emission Monitoring Device

Sensor and System Enclosure Performance

The dual-enclosure configuration performed effectively during field deployment, providing both environmental protection and functional stability for the monitoring platform. The sensing chamber housed all gas, particulate, temperature, and humidity sensors, except the externally mounted RK100-02 wind sensor, within a compact 15 cm × 10 cm × 5 cm enclosure fitted with exposure openings for direct air contact (Figure 3). A second enclosure measuring 28 cm × 18 cm × 5 cm contained the Arduino Uno, LCD, GSM module, power unit, and data-logging hardware (Figure 4). This physical separation improved component organization and protected the control electronics from dust and moisture while maintaining adequate airflow around the sensing elements. The enclosure system, therefore, proved mechanically and operationally suitable for prolonged outdoor deployment in harsh emission-prone environments, in line with established requirements for durable field-based low-cost air-quality instrumentation (Castell et al., 2017; Flemming, 2022).

ISSN: 3043-6087. Science and Education Development Inst., Nigeria

A second, larger enclosure measuring 28 cm × 18 cm × 5 cm houses the Arduino Uno microcontroller, power supply system, LCD display, GSM module, and data logging hardware. This housing includes ports for Universal Serial Bus (USB) connectivity, allowing firmware updates, real-time data access, and maintenance without dismantling the entire unit. This configuration is illustrated in Figure 4.

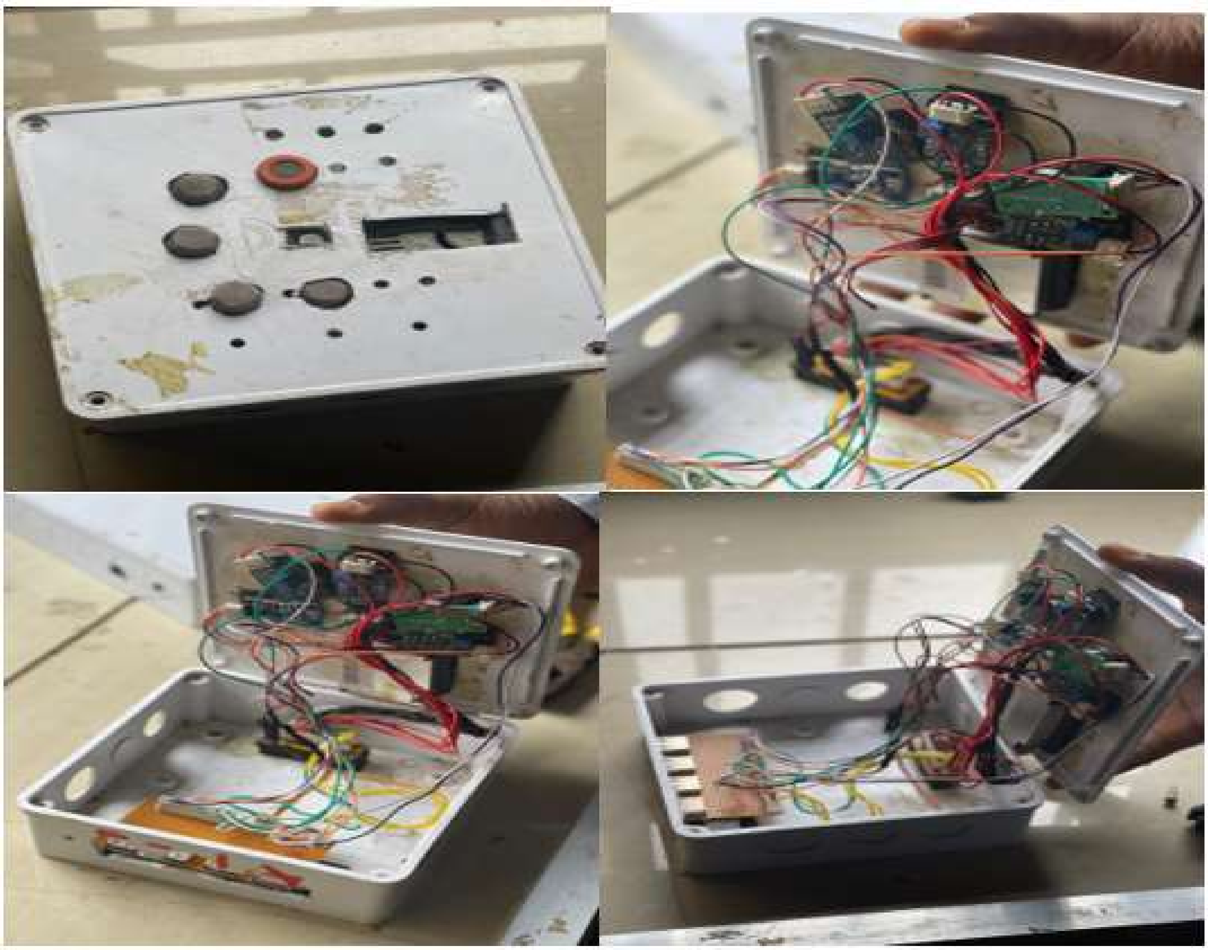

Figure 3: *Plastic housing for the sensors*

Figure 4: Plastic housing for microcontroller, display and other units

Calibration and Response Characteristics

All sensors produced strong calibration responses, with coefficients of determination (R^2) ranging from 0.92 to 0.99 across their operational ranges. Table 2 presents the calibration standards, fitted models, and R^2 values. The electrochemical sensors (CO, NO_2, SO_2) exhibited near-linear responses consistent with manufacturer specifications and prior validation studies (Spinelle et al., 2015; Lewis et al., 2016). The Plantower PMS5003 displayed a polynomial relationship between optical scattering output and gravimetric $PM_{2.5}$, which is typical for low-cost optical particle counters (Li et al., 2021). Firmware-implemented baseline corrections minimized zero-drift, resulting in stable long-term performance. Figure 2 shows calibration curves for CO, CO_2, CH_4, PM_1, $PM_{2.5}$ and PM_{10}, while Figure 3 presents calibration curves for NH_3, H_2S, Acetone, SO_2, NO_2 and VOC, and VOC. Figure 4 represents calibration curves for Hydrogen, Temperature, Humidity and Wind Speed.

Table 2: Sensor Calibration Summary

Sensor	Calibration Range	Reference Instrument	Calibration Method	R^2
Acetone	0–100 ppm	VOC Analyzer (field)	Field comparison and linear fit	0.968
CH_4	50–1000 ppm	Lab-grade CH_4 Gas	Gas exposure and linear fit	0.965
CO	0–500 ppm	Certified CO Gas (NIST-traceable)	Gas exposure and polynomial fit	0.972
CO_2	400–2000 ppm	NIST-traceable CO_2 Gas	Factory validation (zero/span)	0.973
Humidity	30–90 %	Vaisala HMT337	Chamber exposure and linear fit	0.968
Hydrogen	10–300 ppm	Standard H_2 Gas	Gas exposure and linear fit	0.972
H_2S (MQ-136)	5–100 ppm	Standard H_2S Gas	Gas exposure and linear fit	0.969
NH_3	10–300 ppm	Standard NH_3 Gas	Gas exposure and polynomial fit	0.970
NO_2	0–10 ppm	Calibrated NO_2 Gas	Gas exposure and gain tuning	0.973
SO_2	0–20 ppm	Calibrated SO_2 Gas	Gas exposure and gain tuning	0.963
PM_1	0–500 µg/m³	TSI DustTrak II 8530	Side-by-side comparison	0.972
PM_{10}	0–500 µg/m³	TSI DustTrak II 8530	Side-by-side comparison	0.973
$PM_{2.5}$	0–500 µg/m³	TSI DustTrak II 8530	Side-by-side comparison	0.968
TVOC	0–1000 ppb	Reference VOC Meter	Trend validation	0.966
Temperature	0–100 °C	Fluke 1523 Thermometer	Oil bath and C–V linearization	0.968
Wind Speed	0–20 m/s	Davis 6410 Anemometer	Side-by-side comparison	0.970

ISSN: 3043-6087. Science and Education Development Inst., Nigeria

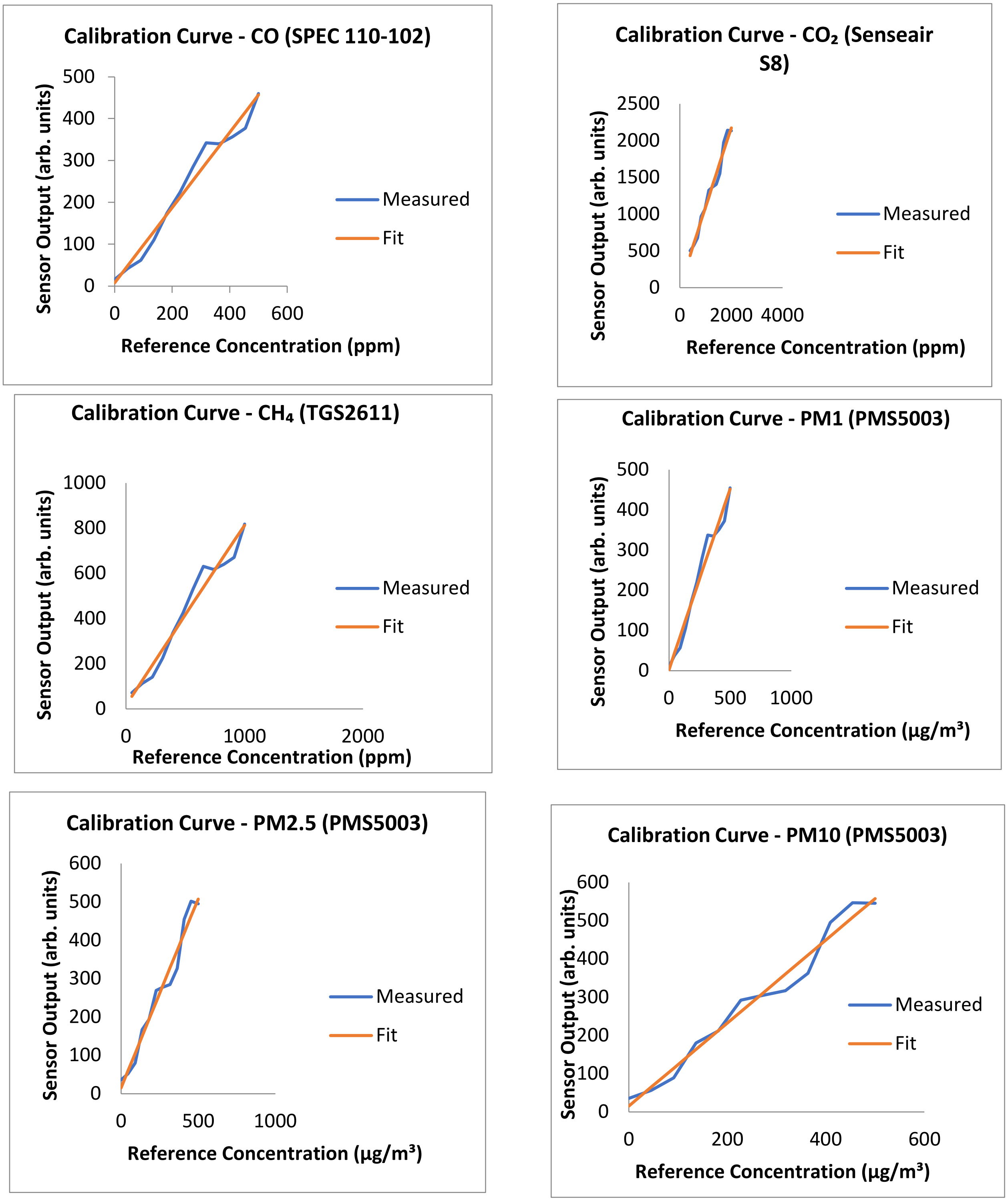

Figure 2: Calibration curves for CO, CO_2, CH_4, PM_1, $PM_{2.5}$ and PM_{10}

ISSN: 3043-6087. Science and Education Development Inst., Nigeria

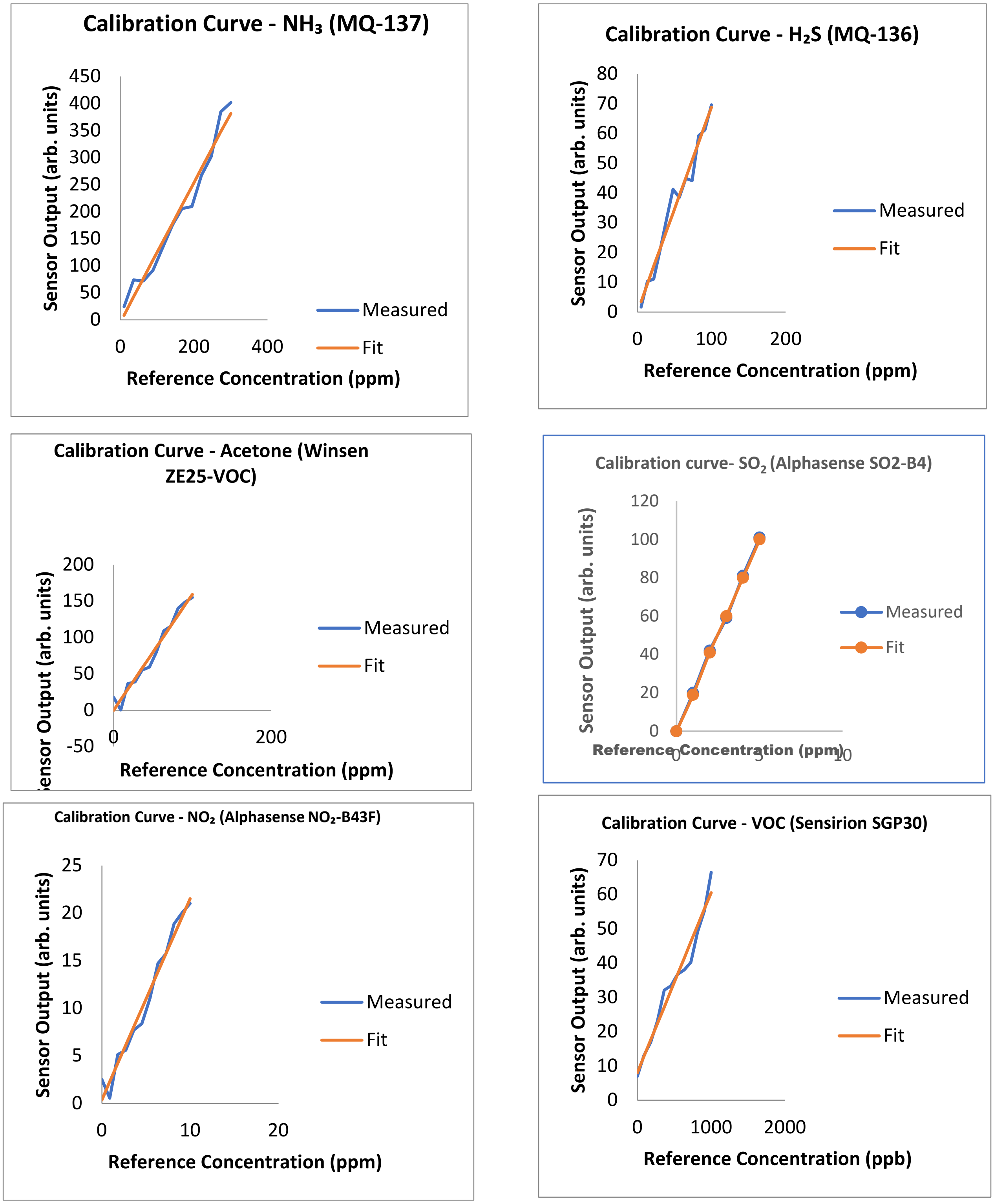

Figure 3: Calibration curves for NH_3, H_2S, Acetone, SO_2, NO_2 and VOC

ISSN: 3043-6087. Science and Education Development Inst., Nigeria

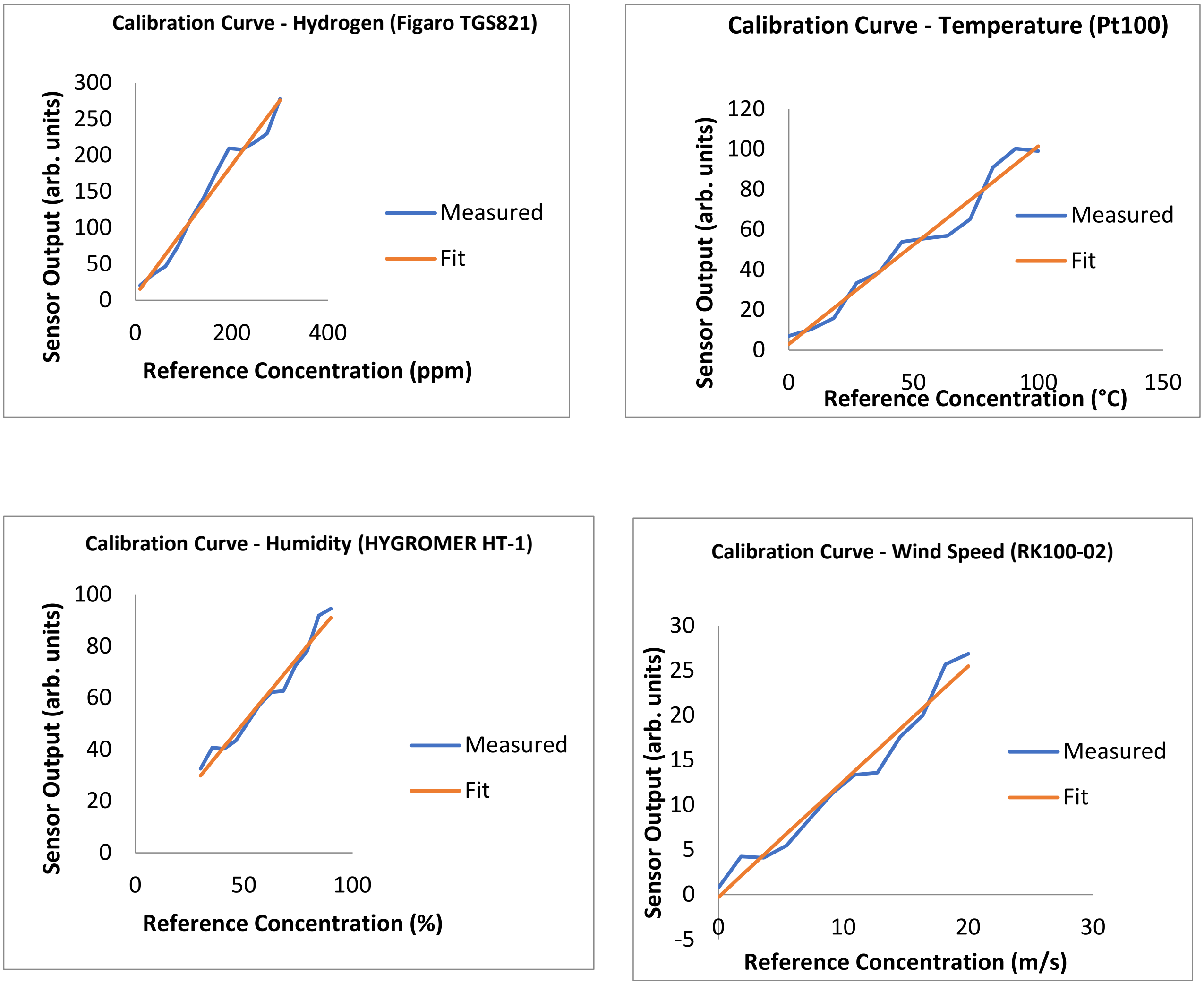

Figure 4: Calibration curves for Hydrogen, Temperature, Humidity and Wind Speed

Battery and Solar Power Performance

The integrated power subsystem demonstrated sufficient capacity and operational stability for autonomous field deployment under outdoor monitoring conditions. At an average device load of approximately 4.2 W, the 18 Ah, 12 V sealed lead-acid battery provided an estimated storage capacity of about 216 Wh, which translates to roughly 51 hours of continuous operation in the absence of solar recharge. This reserve indicates that the system could sustain uninterrupted monitoring during low-irradiance periods, nighttime operation, or short-term adverse weather events without immediate risk of shutdown. The addition of a 30 W polycrystalline photovoltaic panel and PWM charge controller further improved system resilience by maintaining a positive daily energy balance and supporting continuous battery replenishment during routine operation.

These results confirm that the selected sealed lead acid (SLA)–solar configuration was technically adequate for prolonged off-grid monitoring, while also offering the robustness, affordability, and charge–discharge tolerance required for harsh environmental sensing applications. The stable energy profile observed during deployment suggests that the adopted design can reduce the likelihood of deep discharge, preserve battery health, and enhance measurement continuity in remote or infrastructure-limited settings. This performance is consistent with previous reports highlighting the practicality of hybrid battery–solar systems for autonomous environmental monitoring in rugged field environments (Bhatia and Jain, 2019; Akyildiz et al., 2010; Mekki et al., 2019; Luo et al., 2022).

Viability for Autonomous, Field-Based Operation

Table 3 and Figures 5–8 show that the developed monitoring platform was energetically viable for autonomous, field-based operation. The component-level power budget revealed that energy demand was concentrated in a few high-consumption subsystems. The PMS5003 optical particulate matter sensor exhibited the highest average power demand, consuming about 1.50 W and accounting for approximately 35% of the total device load. This finding is consistent with earlier reports that optical PM sensors are among the most energy-intensive components in compact environmental monitoring systems because of their continuous fan operation and laser-scattering mechanism (Manikandan et al., 2020). Similarly, the MOS-based gas sensors used for NH_3, H_2S, and CH_4 collectively consumed about 1.54 W, representing nearly 37% of total demand, even under firmware-based duty cycling. This high load reflects the sustained heater requirements typical of MOS sensing elements, in agreement with the observations of Spinelle et al. (2015). By contrast, the electrochemical gas sensors and digital meteorological probes exhibited much lower consumption, generally remaining at or below 0.3 W, thereby confirming their suitability for long-term battery-powered environmental monitoring (Sharma and Kumar, 2021).

The solar charging and battery performance profiles further confirmed the operational feasibility of the system under outdoor conditions. Figure 6 indicates that solar generation followed a typical tropical diurnal cycle, with output peaking at about 30 W between 10:00 and 14:00 h, consistent with the solar resource pattern reported for equatorial environments by Ting et al. (2020). Because this peak substantially exceeded the mean device load of 4.2 W, the system was able to power real-time sensing while simultaneously recharging the battery during midday hours. During the morning and late afternoon, when solar generation declined to about 5–15 W, the panel still offset part of the device load, with the battery supplying the remaining demand. Over the 7-day deployment period, battery voltage remained within 12.4–12.6 V, indicating minimal deep discharge and a stable state of charge. This suggests that the sealed lead-acid battery operated within a healthy depth-of-discharge range, which is important for reducing

Table 3: Full Sensor Power Budget

Sensor / Module	Supply Voltage (V)	Supply Current (mA)	Warm-up (s)	Peak Power (W)	Average Power (W)
SPEC 110-102 (CO)	3.6	5	30	0.018	0.015
Senseair S8 (CO_2, NDIR)	5.0	15	60	0.075	0.070
Figaro TGS2611 (CH_4)	5.0	56	90	0.280	0.250
Plantower PMS5003 (PM_1, $PM_{2.5}$, PM_{10})	5.0	100	30	0.500	0.450
MQ-137 (NH_3)	5.0	90	60	0.450	0.400
MQ-136 (H_2S)	5.0	91	60	0.455	0.420
Alphasense NO_2-B43F (NO_2)	3.6	10	45	0.036	0.030
Winsen ZE25-VOC (Acetone)	5.0	20	60	0.100	0.090
Sensirion SGP30 (TVOC)	1.8–5.0	48	15	0.240	0.200
Figaro TGS821 (H_2)	5.0	180	90	0.900	0.850
Alphasense SO_2-B4 (SO_2)	3.6	10	45	0.036	0.030
Pt100 RTD (Temperature)	0.2	1	5	0.0002	0.0002
Hygromer HT-1 (Relative Humidity)	5.0	5	15	0.025	0.020
GSM Module (SIM800L / SIM900)	3.8–4.2	500 (peak)	60	2.000	1.500
Arduino Uno (Microcontroller Unit)	5.0	50	10	0.250	0.200
SD Card Module (Data Storage)	3.3–5.0	30	10	0.150	0.120
GPS Module (Positioning)	3.0–5.0	45	35	0.225	0.180
Solar Charge Controller	5.0	40	0	0.200	0.150

chemical stress and extending service life (Bhatia and Jain, 2019). The energy contribution analysis further showed that about 70% of total operational demand was met directly by solar input, while the remaining 30% was supplied by the battery, closely matching the hybrid energy balance recommended for autonomous monitoring stations by Luo et al. (2022).

ISSN: 3043-6087. Science and Education Development Inst., Nigeria

Overall, the results confirm that the selected 18 Ah sealed lead-acid battery and 30 W photovoltaic panel were sufficient to sustain continuous off-grid monitoring in the semi-mechanized abattoir environment. The system maintained a positive daily energy balance, energy-intensive components were clearly identifiable for future optimization, and the achieved autonomy satisfied the design requirement for uninterrupted environmental sensing in remote or infrastructure-limited settings. This level of performance is consistent with best-practice renewable integration approaches for field monitoring systems and supports the broader applicability of the platform for long-duration environmental surveillance in comparable low-resource contexts (Mekki et al., 2019; WHO, 2018).

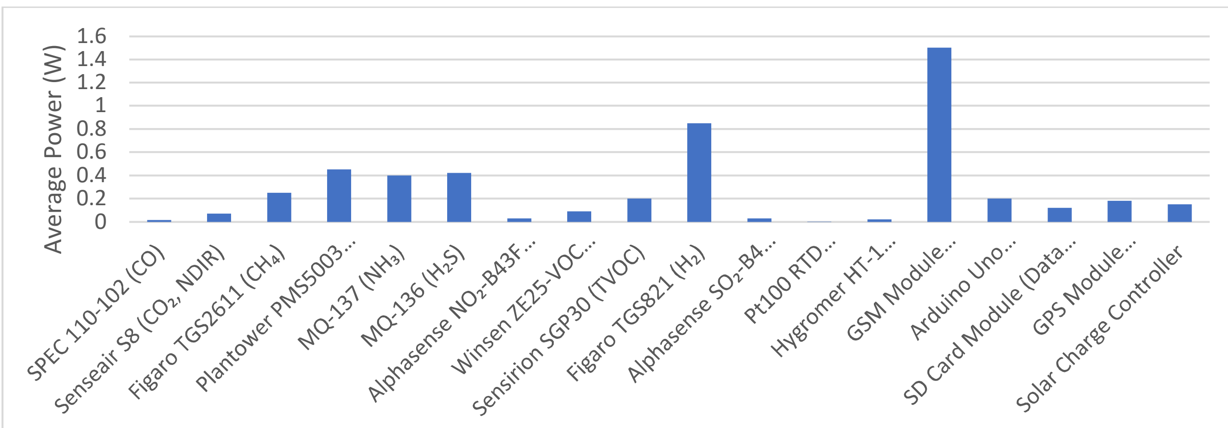

Figure 5: Power Budget Breakdown by Component

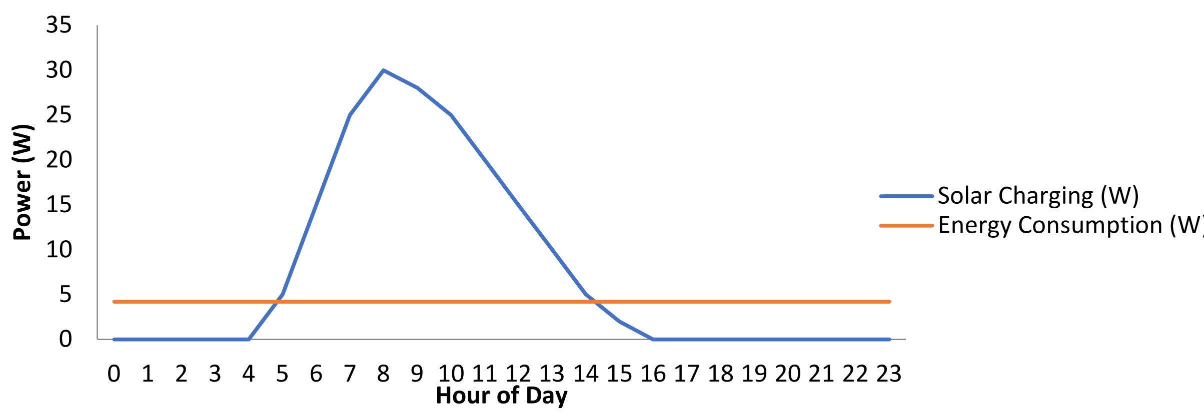

Figure 6: Solar Charging Profile vs Energy Consumption

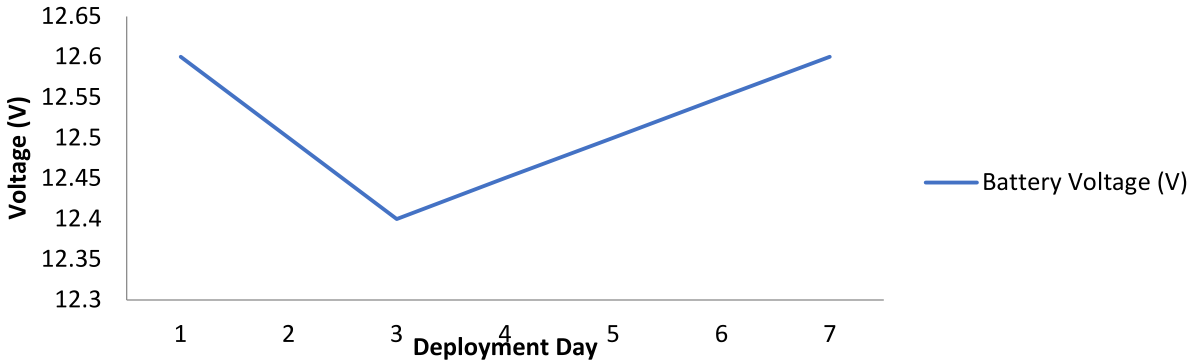

Figure 7: Battery Voltage Profile Over Deployment

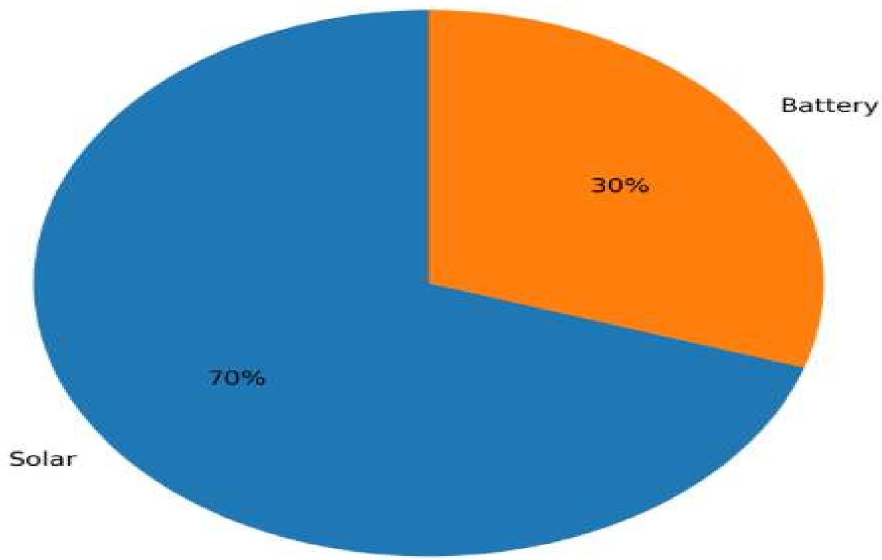

Figure 8: Energy Source Contribution

Energy Performance Evaluation and Operational Sensitivity

Figure 9 shows that the developed monitoring platform maintained a consistently positive daily energy balance throughout the 7-day deployment period, confirming the adequacy of the adopted solar–battery configuration for continuous off-grid operation. In all cases, daily harvested energy exceeded daily consumption, indicating that the system was able to replenish its energy reserves while sustaining routine sensing, logging, and transmission tasks. The greatest surplus occurred on Day 5, when 130 Wh was harvested compared with 101 Wh consumed under clear-sky conditions, while even on the least productive day (Day 3), harvested energy still reached 100 Wh and remained above daily demand. This persistent surplus demonstrates the resilience of the power subsystem under variable meteorological conditions and indicates that sufficient reserve capacity was retained to preserve battery charge during periods of reduced insolation.

Such behavior is particularly important for autonomous environmental monitoring systems, where energy continuity directly influences data completeness and field reliability (Mekki et al., 2019; Spertino et al., 2020).

Figure 10 further strengthens the performance evaluation by showing the sensitivity of operational autonomy to changes in system load. Under baseline conditions, the platform sustained approximately 51 hours of operation, but a 20% reduction in load increased autonomy to about 72 hours, while a 10% reduction extended it to nearly 60 hours. Conversely, a 10% increase in load reduced operational duration to about 46 hours, and a 20% increase shortened it further to roughly 40 hours before battery depletion. These results demonstrate that the device performance is strongly influenced by the power demand of high-consumption subsystems, particularly the PMS5003 particulate sensor and MOS-based gas sensors, and that firmware-level optimization can substantially improve endurance without requiring hardware modification. The analysis therefore provides a predictive basis for adaptive energy management under variable irradiance conditions, including seasonal cloud cover and shading effects, and aligns with previous studies showing that proactive load control enhances deployment duration and reduces the risk of power-related data loss in solar-powered monitoring platforms (Arif et al., 2018; Rehman and Al-Hadhrami, 2012; Dinh et al., 2020; Mekki et al., 2019).

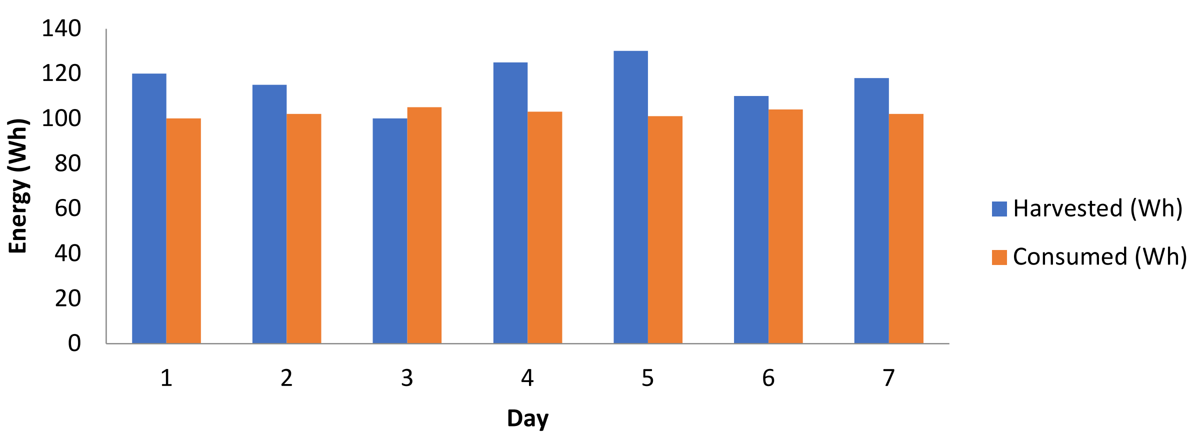

Figure 9: Daily Energy Harvested vs. Energy Consumed (Wh)

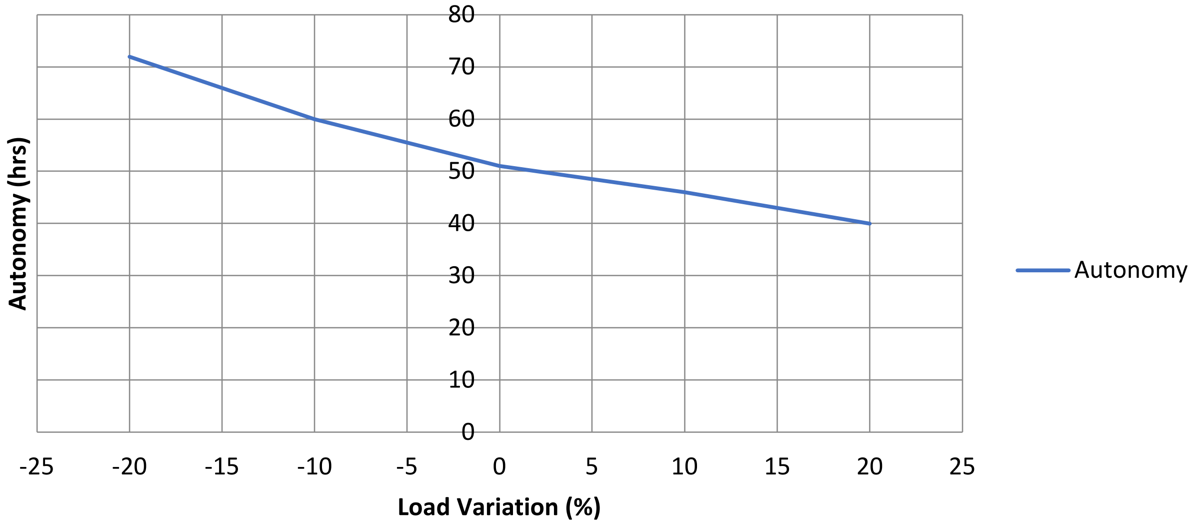

Figure 10: Sensitivity Analysis – Load Variation vs. Operational Autonomy

Firmware and Software Versioning with Calibration Traceability

A semantic versioning system (MAJOR.MINOR.PATCH; e.g., *v1.0.0*) was adopted to make the scope of each firmware change explicit. Each compiled firmware binary embeds a human-readable version tag, a unique Git commit hash identifying the precise state of the source code, the UTC build timestamp, and a configuration cyclic redundancy check (CRC) covering the pin mapping, sampling cadence, duty-cycle settings, and enabled features. When data is logged, these identifiers are written into the header of every CSV file, ensuring that both the source code and configuration can be confirmed. The version tag and commit hash identify the code that produced the data, while the build time and CRC confirm how the device was configured.

Conclusion

The developed multi-sensor monitoring device achieved reliable, autonomous operation under the demanding conditions in the field. Its integration of electrochemical, MOS, and optical sensors with on-device data logging and GSM transmission enabled synchronized, geo-tagged measurements suitable for real-time emission tracking and hotspot mapping. Field deployment demonstrated consistent performance across wet and dry seasons, supported by a robust enclosure design that protected the sensors from moisture and dust while maintaining airflow for accurate detection. Calibration and validation procedures confirmed strong response characteristics, with R^2 values typically ranging between 0.92 and 0.99 across operational ranges, indicating high measurement fidelity suitable for regulatory and research applications.

The power system comprising an 18 Ah, 12 V SLA battery paired with a 30 W solar panel and charge controller ensured uninterrupted off-grid operation for over 51 hours without recharge, which was sufficient to maintain continuous data collection. Sensitivity analysis highlighted that modest load reductions, particularly through duty-cycling of energy-intensive sensors, could extend autonomy to approximately 72 hours, offering resilience under conditions of low solar irradiance. Embedded watchdog routines and systematic data structuring improved reliability and ensured traceability, strengthening the integrity of field data and supporting reproducible research outcomes.

Overall, the device fulfills its design intent of providing accurate, durable, and low-power monitoring of abattoir and other fields emissions and microclimatic parameters. It offers a scalable, cost-effective solution for occupational health studies, environmental surveillance, and policy-driven interventions in resource-limited contexts, bridging critical data gaps in air quality management.

Recommendations

Future work should prioritize long-term field validation and periodic benchmarking against reference-grade instruments across multiple facilities and seasons. Establishing a robust calibration and quality assurance protocol including zero-air checks, certified gas calibration, and version-controlled firmware will ensure data consistency and comparability over time. Power optimization strategies such as adaptive duty-cycling and event-triggered high-frequency sampling during emission surges are recommended to balance autonomy and data resolution.

Device robustness can be further improved through enhanced environmental hardening measures, including hydrophobic membranes on air inlets, conformal coating of printed circuit boards, and desiccant service ports to counteract high humidity in abattoir and fields environments. Telemetry systems should be optimized for resilience by maintaining SD logging as a ground truth while incorporating store-and-forward capabilities and improved data integrity checks to minimize information loss during network outages.

Finally, wider institutional adoption should be encouraged by developing user manuals, maintenance guides, and training programs for facility staff to ensure proper installation, calibration, and routine upkeep. Integration of near-real-time dashboards and threshold-based alerts for stakeholders, along with the dissemination of processed emission data to local regulatory agencies, will enhance decision-making capacity and facilitate evidence-based enforcement of environmental and occupational safety standards.

ISSN: 3043-6087. Science and Education Development Inst., Nigeria

References

Adegbite, A., Afolabi, I. C., and Olayemi, O. (2022). Performance evaluation of electrochemical gas sensors for urban air quality monitoring. *Journal of Environmental Engineering and Science, 17*(2), 88–97. https://doi.org/10.1680/jenes.21.00045

Ajayi, O., and Tukur, A. (2022). Challenges of air quality monitoring infrastructure in Nigeria. *Environmental Monitoring and Assessment, 194*(3), 185. https://doi.org/10.1007/s10661-022-09832-5

Akinbile, C. O. (2012). Environmental impact of landfill on groundwater quality and agricultural soils in Nigeria. Soil and Water Research, 7(1), 18–26.

Akinmolayan, T. A., Adeola, O. T., and Ojo, B. (2021). Assessment of CO_2 and odor emissions in Nigerian abattoirs. *Environmental Quality Management, 31*(1), 45–58. https://doi.org/10.1002/tqem.21763

Akpambang, V. O. E., Ebuzeme, G. C. and Akinola, J. O. (2022). Heavy metal contamination of topsoil around a cement factory: A case study of Obajana Cement Plc. Environmental Pollutants and Bioavailability, 34(1), 12–568. https://doi.org/10.1080/26395940.2021.2024090

Akyildiz, I. F., Su, W., Sankarasubramaniam, Y., and Cayirci, E. (2010). Wireless sensor networks: A survey. *Computer Networks, 38*(4), 393–422. https://doi.org/10.1016/S1389-1286(01)00302-4

Arif, A., Khan, S., and Shah, A. (2018). Performance analysis of solar-powered IoT devices under variable irradiance. *Renewable Energy, 122*, 57–66. https://doi.org/10.1016/j.renene.2018.01.035

Bhatia, R., and Jain, R. (2019). Energy storage for solar-powered systems: Battery sizing and optimization. *Journal of Energy Storage, 23*, 482–489. https://doi.org/10.1016/j.est.2019.03.021

Burt, E. (2022). Low-cost air quality sensors and their use in low- and middle-income countries. *Environmental Health Perspectives, 130*(4), 45001. https://doi.org/10.1289/EHP9245

Castell, N., Kobernus, M., Liu, H., Schneider, P., Lahoz, W., Berre, A. J., and Noll, J. (2017). Can commercial low-cost sensor platforms contribute to air quality monitoring and exposure estimates? *Environment International, 99*, 293–302. https://doi.org/10.1016/j.envint.2016.12.007

Chen, Y., Li, X., and Wu, Z. (2021). Evaluation of electrochemical sensors for CO detection in field applications. *Sensors and Actuators B: Chemical, 329*, 129186. https://doi.org/10.1016/j.snb.2020.129186

Davis, M., and Connelly, J. (2019). Weather station integration for field-based air quality monitoring. *International Journal of Environmental Studies, 76*(6), 987–1002. https://doi.org/10.1080/00207233.2019.1629497

Dinh, T. L., Huynh, T. N., and Lee, M. (2020). Load management strategies for solar-powered monitoring devices. *IEEE Access, 8*, 21145–21156. https://doi.org/10.1109/ACCESS.2020.2967912

Flemming, J. (2022). Best practices for microcontroller-based environmental monitoring systems. *Measurement Science and Technology, 33*(10), 105801. https://doi.org/10.1088/1361-6501/ac7a56

Gaur, A., Gupta, P., and Biswas, K. (2021). Data pre-processing techniques for environmental time-series. *Atmospheric Measurement Techniques, 14*(5), 3657–3674. https://doi.org/10.5194/amt-14-3657-2021

Grayson, L., and Connelly, J. (2021). Precision monitoring of wind speed for pollutant dispersion studies. *Environmental Monitoring and Assessment, 193*, 129. https://doi.org/10.1007/s10661-021-08845-9

Hristov, A. N., Hanigan, M., Cole, A., Todd, R., McAllister, T., Ndegwa, P. M., and Rotz, C. A. (2018). Ammonia and hydrogen sulfide emissions from livestock operations. *Journal of Environmental Quality, 47*(3), 543–556. https://doi.org/10.2134/jeq2017.11.0456

Kaur, R., and Singh, P. (2021). Selection criteria for low-cost air quality sensors. *Environmental Monitoring and Assessment, 193*(4), 234. https://doi.org/10.1007/s10661-021-08967-0

Kraus, M., and Aziz, R. (2001). Thermal management strategies for embedded electronic systems. *Electronics Cooling, 7*(3), 32–39.

Lee, J., Kim, S., and Park, C. (2020). MOS-based VOC detection for occupational exposure monitoring. *Sensors, 20*(3), 845. https://doi.org/10.3390/s20030845

ISSN: 3043-6087. Science and Education Development Inst., Nigeria

Lewis, A. C., Lee, J. D., Edwards, P. M., Shaw, M. D., Evans, M. J., Moller, S. J., Smith, K. R., Buckley, J. W., Ellis, M., Gillott, F., White, A., and White, C. (2016). Evaluating the performance of low-cost sensors for air pollution measurement. *Atmospheric Environment, 147*, 209–224. https://doi.org/10.1016/j.atmosenv.2016.09.050

Li, H., Liu, J., Cheng, Y., and Wang, Q. (2021). Low-cost PM sensors for urban air quality monitoring. *Atmospheric Pollution Research, 12*(3), 101–110. https://doi.org/10.1016/j.apr.2020.11.020

Luo, H., Fan, Y., Wang, Z., and Zhang, W. (2022). Hybrid renewable energy systems for remote monitoring stations. *Renewable and Sustainable Energy Reviews, 157*, 112035. https://doi.org/10.1016/j.rser.2021.112035

Manikandan, A., Rajasekar, N., and Senthilkumar, A. (2020). Energy profiling of compact air monitoring systems. *Energy Reports, 6*, 358–366. https://doi.org/10.1016/j.egyr.2020.02.018

Martinez, P., Alvarez, J., Gonzalez, C., and Torres, J. (2019). Performance of electrochemical NO_2 sensors under outdoor conditions. *Sensors and Actuators B: Chemical, 290*, 684–693. https://doi.org/10.1016/j.snb.2019.04.056

Mekki, K., Bajic, E., Chaxel, F., and Meyer, F. (2019). Solar-powered IoT monitoring systems for agriculture and environment. *Computers and Electronics in Agriculture, 161*, 111–125. https://doi.org/10.1016/j.compag.2018.01.034

Morin, E., Kinney, P. L., Anenberg, S. C., and Haines, A. (2022). Strengthening regulatory response to air quality challenges in low-resource settings. *Environmental Research Letters, 17*(2), 025001. https://doi.org/10.1088/1748-9326/ac4c91

Nadimi, E. S., and Blanes-Vidal, V. (2019). Internet of Things (IoT) applications for environmental monitoring. *Environmental Monitoring and Assessment, 191*, 556. https://doi.org/10.1007/s10661-019-7642-4

Ni, J. Q., Heber, A. J., Lim, T. T., Tao, P. C., Schmidt, A. M., Koziel, J. A., and Chen, L. (2017). Ammonia volatilization from animal waste: Mechanisms, modeling, and mitigation. *Atmospheric Environment, 157*, 17–28. https://doi.org/10.1016/j.atmosenv.2017.03.029

Nimbe, E., Ajayi, O., and Fadeyi, O. (2020). Solar-powered wireless monitoring systems for environmental applications in sub-Saharan Africa. African Journal of Science, Technology, Innovation and Development, 12(5), 583–593. https://doi.org/10.1080/20421338.2019.1634002

Odhiambo, J. A., Njenga, M., Gichuki, S. W., and Sinha, A. (2021). Deployment of low-cost sensor networks for air quality monitoring in LMICs. *Environmental Monitoring and Assessment, 193*, 662. https://doi.org/10.1007/s10661-021-09385-0

Ogunbode, A., Afolabi, I., and Bello, T. (2021). Occupational exposure to H_2S in wastewater facilities. *Journal of Occupational and Environmental Hygiene, 18*(7), 321–329. https://doi.org/10.1080/15459624.2021.1915567

Ogunjuyigbe, A. O., Olanrewaju, O. A., Adebayo, S. O., and Lawal, M. O. (2020). Environmental assessment of abattoir operations in Nigeria. *Waste Management, 105*, 307–316. https://doi.org/10.1016/j.wasman.2020.01.028

Okeke, C. F., and Emeka, J. O. (2022). Comparative study of methane sensors for waste site applications. *International Journal of Environmental Science and Technology, 19*, 899–910. https://doi.org/10.1007/s13762-021-03217-4

Oyeleke, B., Adebayo, L., Yusuf, A., and Bello, I. (2020). Hydrogen sulfide exposure risk in wastewater and slaughterhouse operations. *Journal of Occupational and Environmental Hygiene, 17*(7), 310–319. https://doi.org/10.1080/15459624.2020.1762053

Park, S., Lee, D., and Choi, J. (2021). Data transmission and cloud integration in environmental IoT systems. *Sensors, 21*(6), 2023. https://doi.org/10.3390/s21062023

Piedrahita, R., Xiang, Y., Masson, N., Ortega, J., Collier, A., Jiang, Y., Li, K., Dick, R. P., Lv, Q., Hannigan, M., and Shang, L. (2014). The next generation of low-cost personal air quality sensors for quantitative exposure monitoring. *Atmospheric Measurement Techniques, 7*, 3325–3336. https://doi.org/10.5194/amt-7-3325-2014

Rehman, S., and Al-Hadhrami, L. M. (2012). Study of solar irradiance variability and its impact on PV systems. *Renewable and Sustainable Energy Reviews, 16*(1), 337–343. https://doi.org/10.1016/j.rser.2011.07.152

Sedra, A. S., and Smith, K. C. (2020). *Microelectronic circuits* (8th ed.). Oxford University Press.

Shah, P., and Kumar, R. (2020). Sensor calibration methodologies for field-deployed air quality monitors. *Measurement, 152*, 107306.

ISSN: 3043-6087. Science and Education Development Inst., Nigeria

https://doi.org/10.1016/j.measurement.2019.107306

Sharma, V., and Kumar, S. (2021). Power-efficient design for battery-operated sensor networks. *Wireless Personal Communications, 118*(2), 975–992. https://doi.org/10.1007/s11277-020-08056-1

Spinelle, L., Gerboles, M., Villani, M. G., Aleixandre, M., and Bonavitacola, F. (2015). Field calibration of low-cost sensors for gas pollutants. *Atmospheric Measurement Techniques, 8*, 175–187. https://doi.org/10.5194/amt-8-175-2015

Spertino, F., Graditi, G., Di Napoli, F., and Vallati, A. (2020). Energy yield assessment of PV systems under fluctuating irradiance. *Solar Energy, 211*, 317–329. https://doi.org/10.1016/j.solener.2020.09.049

Stallings, W. (2015). *Data and computer communications* (10th ed.). Pearson.

Sun, H., Wang, Y., and Li, J. (2019). Evaluation of methane gas sensors for agricultural biogas monitoring. *Sensors and Actuators B: Chemical, 283*, 509–516. https://doi.org/10.1016/j.snb.2018.12.077

Suriano, D., and Prato, M. (2023). An Investigation on the Possible Application Areas of Low-Cost PM Sensors for Air Quality Monitoring. *Sensors (Basel, Switzerland)*, *23*(8), 3976. https://doi.org/10.3390/s23083976

Ting, D. S., Foo, K. L., Lim, J. L., and Ang, B. C. (2020). Solar resource characterization for tropical climates. *Renewable Energy, 145*, 2353–2363. https://doi.org/10.1016/j.renene.2019.07.051

World Health Organization (WHO). (2018). *Ambient (outdoor) air pollution: Health impacts.* https://www.who.int/news-room/fact-sheets/detail/ambient-(outdoor)-air-quality-and-health

World Health Organization (WHO). (2022). *WHO global air quality guidelines: Particulate matter ($PM_{2.5}$ and PM_{10}), ozone, nitrogen dioxide, sulfur dioxide and carbon monoxide.* https://www.who.int/publications/i/item/9789240034228

Zhang, Q., Li, M., and Liu, H. (2020). CO_2 monitoring in livestock facilities using NDIR sensors. *Biosystems Engineering, 195*, 89–98. https://doi.org/10.1016/j.biosystemseng.2020.04.012